Earth **Surface**
Dynamics
Discussions

1 **Short communication: Field data imply that the sorting (D96/D50 ratios) of gravel bars in**

2 **coarse-grained streams influences the probability of sediment transport**

3

4 **Running title: transport probability of coarse-grained material**

5

6 *Fritz Schlunegger, Romain Delunel and Philippos Garefalakis*

7 Institute of Geological Sciences, University of Bern, 3012 Bern, Switzerland

8 +41 31 631 8767, schlunegger@geo.unibe.ch

9

10 **Abstract**

11 Conceptual models suggest that the mobility of fluvial gravel bars is mainly controlled by

12 sediment discharge. Here we present field observations from streams in the Swiss Alps and the

13 Peruvian Andes to document that for a given water runoff, the probability of bedload transport

14 also depends on the sorting of the bed material. We calculate shear stresses that are expected

15 for a mean annual water discharge, and compare these estimates with grain-specific thresholds.

16 We find a positive correlation between the predicted probability of transport and the sorting of the

17 bed material, expressed by the D_{96}/D_{50} ratio. These results suggest that besides sediment discharge,

18 the bedload sorting exerts a measurable control on the gravel bar mobility.

19

20 **1   Introduction**

21 The dynamics and the mobility of gravel bars in coarse-grained streams exert a strong control on the

22 channel form, where a large gravel bar mobility is commonly found in braided rivers, while a low

23 mobility is associated with more stable channels (Church, 2006). Flume experiments (Dietrich et al.,

24 1989) and numerical models (Wickert et al., 2013) have shown that sediment flux is one of the most

25 important parameters, which controls the dynamics of these bars (Dade and Friend, 1998; Church,

26 2006) and which leaves a measurable impact in fluvial stratigraphies (Allen et al., 2013).

27 Accordingly, a large sediment flux would increase the mobility of gravel bars and promote streams

28 to adapt a braided pattern. In contrast, a low sediment flux is predicted to result in an armoring of

29 the channel floor (Carling, 1981; Aberle and Nikora, 2006) through selective entrainment of finer-

30 grained sediments (Whiting et al., 1988; Dietrich et al., 1989), thereby resulting in a better sorting

31 of the channel bed material and in a stabilization and confinement of the channel-bar arrangement

32 (Church, 2006). If this hypothesis was correct, one would also expect that well-sorted gravel bars

33 should be less frequently reworked than poorly sorted one (Whiting et al., 1988), and that braided

34 streams host gravel bars with a higher mobility probability than confined rivers. Here, we test this

35 hypothesis with a focus on gravelly streams in the Swiss Alps where flow is confined in

36 artificial channels, and in the Peruvian Andes where streams are braided. We selected gravel

37 bars close to water gauging stations, determined the grain size distribution of these bars and

38 calculated the probability of sediment transport for a selected water runoff, which in our case

39 corresponds to the mean annual water discharge for comparison purposes. We explored whether

40   these flows are strong enough to shift the clasts that build the sedimentary framework of these

41   bars. We thus considered the mobilization of these clasts as a condition, and thus as a threshold,

42   for a change in the sedimentary arrangement of the target gravels bars. The braided character of

43   streams in Peru complicates the calculation of the sediment transport probability mainly

44   because of the large variability in channel widths and the occurrence of multiple active

45   channels within a reach. For these streams, we therefore focused on a segment where all water

46   flows in one single channel with a constant width over a c. 100 m-long reach. The research sites

47   therefore offered conditions that are similar, or close, to a laboratory flume experiment (e.g.,

48   Dietrich et al., 1989) where channel metrics (width and gradient) are nearly stable, and where

49   sediment transport, conditioned by grain size specific thresholds, mainly depends on water

50   runoff and the related flow strength.

51

52   **2   Methods and datasets**

53   *2.1   Entrainment of bedload material, and probability of sediment transport*

54   Sediment mobilization occurs when flow strength τ exceeds a grain size specific threshold τ_c (e.g.,

55   Paola et al., 1992):

56    $\tau > \tau_c$ (1).

57   Threshold shear stress τ_c for the dislocation of grains with size D_x can be obtained using Shields

58   (1936) criteria ϕ for the entrainment of sediment particles:

59    $$\tau_c = \phi(\rho_s - \rho)gD_x$$ (2),

60   where g denotes the gravitational acceleration and ρ_s and ρ the sediment and water densities,

61   respectively. Assignments of values to ϕ vary and diverge between flume experiments (e.g.,

62   Carling et al., 1992; Ferguson, 2012; Powell et al., 2016) and field observations (Mueller et al.,

63   2005; Lamb et al., 2008). We employ the full range between 0.03 and 0.06 (Dade and Friend, 1998),

64   which considers most of the complexities including hiding and protrusion effects that are associated

65   with sediment transport of coarse-grained material (e.g., Buffington and Montgomery, 1997;

66   Whitaker and Potts, 2007; Wickert et al., 2013; Powell et al., 2016). It also accounts for the slope

67   dependency of ϕ for most of the cases particularly where energy gradients are flatter than c. 0.01

68   (Bunte et al., 2013), as is generally the case here with a few exceptions (Table 1). Among the

69   various grain sizes, the 84th percentile D_{84} has been considered to best characterize the sedimentary

70   framework of a gravel bar (Howard, 1980; Hey and Thorne, 1986; Grant et al., 1990). Accordingly,

71   flows that dislocate the D_{84} grain size are strong enough to alter the gravel bar architecture (Grant et

72   al., 1990). We thus selected this threshold to quantify the minimum flow strengths τ_c to entrain the

73   bed material. The use of the D_{50} (e.g., Paola and Mohrig, 1996) would yield in a lower threshold and

74   thus in a greater transport probability.

75   Bed shear stress τ is computed through (e.g., Tucker and Slingerland, 1997):

76    $$\tau = \rho gRS$$ (3).

77   Here, S denotes the energy gradient, and R is the hydraulic radius, which is approximated

78   through water depth d where channel widths $W > 20 \times d$ (Tucker and Slingerland, 1997), which

79   is the case here. The combination of expressions for: (i) the continuity of mass including flow

80   velocity V, channel width W and water discharge Q:

81   $$Q = VWd \tag{4};$$

82   (ii) the relationship between flow velocity and channel bed roughness n (Manning, 1891):

83   $$V = \frac{1}{n} d^{2/3} S^{1/2} \tag{5};$$

84   and (iii) an equation for the Manning's roughness number n (Jarrett, 1984):

85   $$n = 0.32 S^{0.38} d^{-1/6} \tag{6};$$

86   yields a relationship where bed shear stress τ depends on gradient, water flux and channel width

87   (Litty et al., 2017):

88   $$\tau = 0.54 \rho g \left(\frac{Q}{W} \right)^{0.55} S^{0.935} \tag{7}.$$

89   This equation is similar to the expression by Hancock and Anderson (2002), Norton et al.

90   (2016) and Wickert and Schildgen (2019) with minor differences regarding the exponent on the

91   channel gradient S and on the ratio Q/W. These mainly base on the different ways of how bed

92   roughness is considered. The results, however, are similar.

93   We propagated the uncertainties in the variables (Table 1) using Monte Carlo simulations.

94   Simulations were repeated 10'000 times, and the results are reported as percentage where $\tau > \tau_c$

95   during these iterations. These values then represent probabilities of sediment transport for a given

96   water discharge.

97

98   *2.2   Datasets*

99   We collected grain size data from streams where water discharge has been monitored during the

100   past years. These are the Kander, Lütschine, Rhein, Sarine, Simme, Sitter and Thur Rivers in

101   the Swiss Alps (Fig. 1a). The target gravel bars are situated close to a water gauging station. At

102   these sites, digital photographs were taken along or across a gravel bar with a Canon EOS PR.

103   Grain sizes were measured with the Wolman (1954) method using the free software package

104   ImageJ 1.52n (https://imagej.nih.gov). Following Wolman (1954), we used intersecting points

105   of a grid to randomly select the grains to measure. A digital grid of 20x20 cm was thus placed

106   on each photograph with its origin placed at the lower left corner of the photo. The intermediate

107   or *b*-axis of approximately 250 – 300 grains situated beneath an interception point was

108   measured at each location (gravel bar). In cases where more than half of the grain is buried, the

109   neighboring grain was measured instead. If the same grain lay beneath several interception

110   points, then the grain was only measured once. Only grains larger than a few millimeters could

111   be measured. We complemented these data sets with published information on the D_{50}, D_{84} and

112   D_{96} grain size (Litty and Schlunegger, 2017; Litty et al., 2017) for further streams in

113 Switzerland and Peru (Figs. 1a and 1b; Table 1). These authors used the same approach upon

114 collecting grain size data, which justifies the combination of the new with the published

115 datasets.

116 For the Swiss streams, channel widths and gradients (Table 1) were measured on orthophotos

117 and LiDAR DEMs with a 2-m resolution provided by Swisstopo. We complemented this

118 information with published values for channel width estimates for 21 Peruvian streams and for

119 additional 5 streams in Switzerland (Table 1, please see references there). We added a 20%

120 uncertainty on the morphometric variables, which considers the natural variability in gradients

121 and channel widths along the study reaches. We likewise assigned an uncertainty of 20% to the

122 grain size dataset, which considers a possible bias that could be related to the grain size

123 measuring techniques (e.g., sieving in the field versus grain size measurements using the

124 Wolman method; Watkins, 2019). It also considers a mean estimate for the temporal variability

125 in the grain size data, as a repeated measurement on selected gravel bars in Switzerland has

126 shown (Hauser, 2018). We considered that the Shields variable ϕ is equally distributed between

127 0.03 and 0.06 during the 10'000 iterations.

128 The Federal Office for the Environment (FOEN) of Switzerland has measured the runoff values

129 of Swiss streams over several decades. We employed the mean annual discharge values over 20

130 years for these streams and calculated one standard deviation thereof (see Table 1). For the

131 Peruvian streams, water discharges reported by Litty et al. (2017 and Reber et al. (2017) were

132 used.

133

134 **3   Results**

135 The grain sizes range from 8 mm to 70 mm for the D_{50}, 29 mm to 128 mm for the D_{84}, and 52 mm

136 and 263 mm to the D_{96}. The smallest and largest D_{50} values were determined for the Maggia and

137 Rhein Rivers in the Swiss Alps, respectively (Table 1). The grain sizes in the Swiss Rivers also

138 reveal the largest spread where the ratio between the D_{96} and D_{50} grain size ranges between 2.2

139 (Sarine) and 17.7 (Maggia Losone I), while the corresponding ratios in the Peruvian streams are

140 between 2.1 (PRC-ME9) and 5.8 (PRC-ME17). In the Swiss Alps, the critical shear stresses τ_c

141 (median values) for entraining the D_{84} grain size ranges from c. 20 Pa (Emme River) to c. 90 Pa

142 (Rhein and Simme Rivers). In the Peruvian Andes, the largest critical shear values are <80 Pa

143 (PRC-ME39). The shear stress values related to the mean annual water discharge (Q_{med}) range from

144 c. 15 Pa to 100 Pa in the Alps and from 20 Pa to >400 Pa in the Andes. Considering the strength of

145 a mean annual flow and the D_{84} grain size as threshold, the probability of sediment transport

146 occurrence in the Peruvian Andes and in the Swiss Alps comprises the full range between 0% and

147 100%.

148 Rivers that are not affected by recurrent high magnitude events (e.g., debris flows) and where

149 the grain size distribution is not perturbed by lateral material supply are expected to display a self-

150 similar grain size distribution (Whittaker et al., 2011; D'Arcy et al., 2017; Harries et al., 2018),

151   characterized by a linear relationship between the D_{84}/D_{50} and D_{96}/D_{50} ratios. In case of the Maggia

152   River, the largest grains are oversized if the D_{50} and the grain size distribution of the other streams

153   are considered as reference (Fig. 2). This could either reflect a response to the high magnitude

154   floods in this stream (Brönnimann et al., 2018), or to the supply of coarse-grained material by a

155   tributary stream where the confluence is <1 km upstream of the Maggia sites. If we exclude the

156   Maggia dataset, then the probability of sediment transport occurrence scales positively and linearly

157   with the D_{96}/D_{50} ratios (Fig. 3). The observed relationship appears stronger for the Swiss rivers (R^2 =

158   0.74, p-value = 2E-4) than for the Peruvian stream (R^2 = 0.33, p-value = 4E-3). These correlations

159   suggest that gravel bars with a poorer sorting of the bedload, here expressed by a high D_{96}/D_{50} ratio,

160   have a greater probability for the occurrence of sediment transport than those with better-sorted

161   material. Figure 3 also shows that for a given material sorting, the mobilization probability is

162   greater in the Peruvian than in the Swiss rivers.

163

164   **4   Discussion and Conclusions**

165   The sediment transport calculation is based on the inference that floods are strong enough to entrain

166   the frame building grain size D_{84}. Therefore, the relationships between the mobilization probability

167   and the D_{96}/D_{50} ratio could depend on the selected grain size percentile (e.g., the D_{84} versus the D_{50}),

168   which sets the transport threshold. However, this variable linearly propagates into the equation (2)

169   and thus into the probability of $\tau > \tau_c$. Therefore, although the resulting probabilities vary depending

170   on the threshold grain size, the relationships between the D_{96}/D_{50} ratio and the mobilization

171   probability will not change. For the case where different discharge estimates are considered, here

172   expressed as the ratio Δ of a specific runoff to the mean annual discharge Q_{med}, then the

173   corresponding probability of sediment transport will change by $\sim \sqrt{\Delta}$ (equation 7), but the

174   dependency on the D_{96}/D_{50} ratio will remain. This suggests that the sorting of the bed material has a

175   measurable impact on the mobility of gravel bars and thus on the frequency of sediment

176   mobilization irrespective of the selection of a threshold grain size and the choice of a reference

177   water discharge. We note that while the data is relatively scarce and scattered (i.e., the same

178   transport probability for c. twofold difference in the D_{96}/D_{50} ratio), the relationships observed

179   between the probability of transport occurrence and the degree of material sorting are significant

180   with p-values <<0.01. We explain the scatter in the data by the natural stochastic nature of

181   processes that are commonly encountered in the field.

182   For a given D_{96}/D_{50} ratio, the probability of material transport is greater in the Peruvian than in the

183   Swiss rivers. We explain this by the differences in the geomorphic conditions and sediment supply

184   processes between both mountain ranges, and by the anthropogenic corrections of the Swiss streams.

185   In the Swiss Alps, the channel network, the processes on the hillslopes, and the pattern of erosion

186   and sediment supply has mainly been conditioned, and thus controlled, by the glacial impact on the

187   landscape and the large variability of exposed bedrock lithologies (Salcher et al., 2014;

188   Stutenbecker et al., 2016). In contrast, the erosion and sediment supply in the western Peruvian

189   Andes is mainly driven by the combined effect of orographic rain (Montgomery et al., 2001; Viveen

190   et al., 2019) and earthquakes (McPhilips et al., 2014). Because the patterns, conditions and

191   mechanisms of sediment supply largely influence the grain size distribution of the supplied material

192   (Attal et al., 2015), and as consequence, the downstream propagation of these grain size signals

193   (Sklar et al., 2006), we do not expect identical relationships between grain size parameters and

194   probability of sediment transport in both mountain ranges. In addition, all streams in Switzerland

195   are confined in artificial channels with a limited possibility for lateral shifts of gravel bars. The

196   confinement of runoff in artificial channels could thus enhance the armoring effect (Aberle and

197   Nikora, 2006), with the consequence that the sediment transport probability for a given flow

198   strength is likely to decrease, also because armoring results in a successive coarsening of the

199   material and in larger thresholds. Accordingly, the low sediment transport probability in the Alps

200   might have an anthropogenic cause, but a confirmation warrants further research. In Peru, channels

201   are braided within a broad channel belt. Therefore, the probability of a change in the bar-channel

202   arrangement is expected to be higher than in the confined Swiss streams. Despite these differences,

203   we predict that the sorting of coarse-grained bed sediments has measurable impacts on the mobility

204   of the bedload material. We therefore suggest that besides grain size, channel gradient, sediment

205   flux and transport regime (Dade and Friend, 1998; Church, 2006), the sorting of the bed material

206   represents an additional, yet important variable that influences the mobility of the gravel bars and

207   thus the stability of channels.

208

209   Figure 1

210   A) Map showing the sites where grain size data has been measured in the Swiss Alps. The research

211   sites are close to water gauging stations; B) map showing locations for which grain size and water

212   discharge data is available in Peru (Litty et al., 2017).

213

214   Figure 2

215   Relationship between ratio of the D_{96}/D_{50} and D_{84}/D_{50}, implying that the D_{96} grain sizes of the

216   Maggia gravel bars are too large if the D_{50} is taken as reference and if the other gravel bars are

217   considered.

218

219   Figure 3

220   Relationships between the probability of sediment transport occurrence and the D_{96}/D_{50} ratio, which

221   we use as proxy for the sorting of the gravel bar, in the Swiss and Peruvian rivers.

222

223   Table 1

224   Channel morphometry (width and gradient), grain size and water discharge measured at the research

225   sites. The table also shows the results of the various calculations (critical shear stress τ_c, shear stress

226   τ of a flow with a mean annual runoff Q_{med}, and probability of sediment transport occurrence related

Earth **Surface**
Dynamics
Discussions

227 to this flow).

228

229 **Acknowledges**

232

233 **References**

234 Aberle, J. and Nikora, V.: Statistical properties of armored gravel bed surfaces, Water Resour. Res,
235   42, W11414, 2006.
236 Allen, P.A., Armitage, J.J., Carter, A., Duller, R.A., Michael, N.A., Sinclair, H.D., Whitchurch,
237   A.L., and Whittaker, A.C.: The Qs problem: Sediment balance of proximal foreland basin
238   systems, Sedimentology, 60, 102-130, 2013.
239 Attal, M., Mudd, S.M., Hurst, M.D., Weinmann, B., Yoo, K., and Naylor, N.: Impact of change in
240   erosion rate and landscape steepness on hillslopes and fluvial sediments grain size in the
241   Feather River basin (Sierra Nevada, California), Earth Surf. Dyn., 3, 201-222, 2015.
242 Bunte, K., Abt, S.R., Swingle, K.W., Cenderelli, D.A., and Schneider, M.: Critical Shields values in
243   coarse-bedded steep streams, Water Res. Res., 49, 7427-7447, 2013.
244 Brönninmann, S., et al.: 1968 – das Hochwasser, das die Schweiz veränderte. Ursachen, Folgen und
245   Lehren für die Zukunft, Geographica Bernensai, G94, 52 p., 2018
246 Buffington, J. M. and Montgomery, D. R.: A systematic analysis of eight decades of incipient
247   motion studies, with special reference to gravel-bedded rivers, Water Resour. Res., 33,
248   1993-2029, 1997.
249 Church, M.: Bed material transport and the morphology of alluvial river channels, Ann. Rev. Earth
250   Planet. Sci., 34, 325-354, 2006.
251 Carling, P. A.: Armored versus paved gravel beds – discussion, J. Hydraul. Div., 107, 1117–1118,
252   1981.
253 Carling, P. A., Kelsey, A., and Glaister, M. S.: Effect of bed rough- ness, particle shape and
254   orientation on initial motion criteria, in: Dynamics of gravel-bed rivers, edited by: Billi, P.,
255   Hey, R. D., Throne, C. R., and Tacconi, P., 23–39, John Wiley and Sons, Ltd., Chichester,
256   1992.
257 D'Arcy, M., Whittaker, A.C., and Roda-Bolduda, D.C.: Measuring alluvial fan sensitivity to past
258   climate changes using a self-similarity approach to grain-size fining, Death Valley,
259   California, Sedimentology, 64, 388-424, 2017.
260 Dade, B. and Friend, P.F.: Grain-size, sediment-transport regime, and channel slope in alluvial
261   rivers, J. Geol., 106, 661-676, 1988.
262 Dietrich, W.E., Kirchner, J.W., Hiroshi, I., and Iseya, F.: Sediment supply and the development of
263   the coarse surface layer in gravel-bedded rivers, Nature, 340, 215-217, 1989.
264 Ferguson, R.: River channel slope, flow resistance, and gravel entrainment thresholds, Water
265   Resources Research, 48, W05517, 2012.
266 Grant, G. E., Swanson, F. J., and Wolman, M. G.: Pattern and origin of stepped-bed morphology in
267   high gradient streams, western Cascades, Oregon, GSA Bull., 102, 340–352, 1990.
268 Hancock, G.S., and Anderson, B.S.: Numerical modeling of fluvial strath-terrace formation in
269   response to oscillating climate, GSA Bull., 9, 1131-1142, 2002.
270 Harries, R.M., Kirstein, L.A., Whittaker, A.C., Attal, M., Peralta, S., and Brooke, S.: Evidence for
271   self-similar bedload transport on Andean alluvial fans, Iglesia, basin, South Central
272   Argentina, J. Geophys. Res. - Earth Surface, 123, 2292-2315, 2018.
273 Hauser, R.: Abhängigkeit von Korngrössen und Flussformen in den Schweizer Alpen, Unpubl.
274   Ms thesis, Univ. Bern, Bern, Switzerland, 64 p., 2018.

275   Hey, R. D. and Thorne, C. R.: Stable channels with mobile gravel beds, J. Hydrol. Eng., 112, 671–
276   689, 1986.
277   Howard, A. D.: Threshold in river regimes, in: Thresholds in geomorphology, edited by: Coates,
278   D.R, and Vitek, J.D., Allen and Unwin, Boston, MA, 227-258, 1980.
279   Jarrett, R. D.: Hydraulics of high-gradient streams, J. Hydraul. Eng., 110, 1519-1939, 1984.
280   Lamb, M. P., Dietrich, W. E., and Venditti, J. G.: Is the critical Shields stress for incipient sediment
281   motion dependent on channel bed slope? J. Geophys. Res., 113, F02008, 2008.
282   Litty, C. and Schlunegger, F.: Controls on pebbles' size and shape in streams of the Swiss Alps, J.
283   Geol., 125, 101-112, 2017.
284   Litty, C., Schlunegger, F., and Viveen, W.: Possible threshold controls on sediment grain properties
285   of Peruvian coastal river basins, Earth Surf. Dyn., 5, 571-583, 2017.
286   Manning, R.: On the flow of water in open channels and pipes, Trans. Inst. Civil Eng. Ireland, 20,
287   161–207, 1891.
288   McPhilips, D., Bierman, P.R., and Rood, D.H.: 2014, Millennial-scale record of landslides in the
289   Andes consistent with earthquake trigger, Nature Geosci., 7, 925-930, 2014.
290   Montgomery, D. R., Balco, G., and Willett, S. D.: Climate, tectonics, and the morphology of the
291   Andes, Geology, 29, 579–582, 2001.
292   Mueller, E. R., Pitlick, J., and Nelson, J. M.: Variation in the reference Shields stress for bed load
293   transport in gravel- bed streams and rivers, Water Res. Res., 41, W04006, 2005.
294   Norton, K.P., Schlunegger, F., and Litty, C.: On the potential for regolith control of fluvial terrace
295   formation in semi-arid escarpments, Earth Surf. Dyn., 4, 147-157, 2016.
296   Paola, C., Heller, P.L., and Angevine, C.: The large-scale dyanmics of grain size variation in
297   alluvial basins, 1: Theory, Basin Res., 4, 73-90, 1992.
298   Paola, C. and Mohring, D.: Palaeohydraulics revisted: palaeoslope estimation in coarse-grained
299   braided rivers, Basin Res., 8, 243-254, 1996.
300   Powell, M. D., Ockleford, A., Rice, S. P., Hillier, J. K., Nguyen, T., Reid, I., Tate, N. J., and
301   Ackerley, D.: Structural properties of mobile armors formed at different flow strengths in
302   gravel-bed rivers, J. Gephys. Res. – Earth Surface, 121, 1494-1515, 2016.
303   Reber, R., Delunel, R., Schlunegger, F., Litty, C., Madella, A., Akcar, N., and Christl, M.:
304   Environmental controls on 10Be-based catchment-averaged denudation rates along the
305   western margin of the Peruvian Andes, Terra Nova, 29, 282-293, 2017.
306   Salcher, B.C., Kober, F., Kissling, E., and Willett, S.D.: Glacial impact on short-wavelength
307   topography and long-lasting effects on the denudation of a deglaciated mountain range,
308   Global Planet. Change, 115, 59-70, 2014.
309   Shields A.: Anwendung der Ahnlichkeitsmekanik und der Turbulenzforschung auf die
310   Geschiebebewegung, Mitt. Preuss. Versuch. Wasserbau Schiffbau, 26 p., Berlin, 1936.
311   Sklar, L.S., Dietrich, W.E., Foufoula-Georgiou, E.F., Lashermes, B., and Bellugi, D.: 2006, Do
312   gravel bed river size distributions record channel network structure?, Water Res. Res., 42,
313   W06D18, 2006.
314   Stutenbecker, L., Costa, A., and Schlunegger, F.: Lithological control on the landscape form from
315   the upper Rhône Basin, Central Swiss Alps, Earth Surf. Dyn., 4, 253-272, 2016.
316   Tucker, G., and Slingerland, R.: Drainage basin responses to climate change, Water Res. Res, 33,
317   2031-2047, 1997.
318   Viveen, W., Zellavos-Valdivia, L., and Sanjurjo-Sanchez, J.: The influence of centennial-scale
319   variations in the South American summer monsoon and base-level fall on Holocene
320   fluvial systems in the Peruvian Andes, Gobal Planet. Change, 176, 1.22, 2019.
321   Watkins, S.: Linking source and sink in an active rift: quantifying controls on sediment export and
322   depositional stratigraphy in the Gulf of Corinth, Central Greece, PhD thesis, Imperial
323   College London, London, UK, 213 p., 2019.
324   Whitaker, A., and Potts, D.F.: Analysis of flow competence in alluvial gravel bed stream, Dupuyer

Earth **Surface**
Dynamics
Discussions

325   Creek, Montana, Water Res. Res., 43, W07433.
326   Whiting, P. J., Dietrich, W. E., Leopold, L. B., Drake, T. G., and Shreve, R. L.: Bedload sheets in
327   heterogeneous sediment, Geology, 16, 105-108, 1988.
328   Whittaker, A.C., Duller, R.A., Springett, J., Smithells, R.A., Whitchurch, A.L., and Allen, P.A.:
329   Decoding downstream trends in straigraphic grain size as a function of tectonic subsidence
330   and sediment supply, GSA Bull., 123, 1363-1382, 2011.
331   Wickert , A.D., Martin, J.M., Tal, M., Kim, W., Sheets, B., and Paola, C.: River channel lateral
332   mobility: metrics, time scales, and controls, J. Geophys. Res. - Earth Surface, 118, 396-
333   412, 2013.
334   Wickert, A.D., and Schildgen, T.F.: Long-profile evolution of transport-limited gravel-bed rivers,
335   Earth Surf. Dyn, 7, 17-43, 2019.
336   Wolman, M. G.: A method of sampling coarse riverbed material, Eos Trans AGU, 35, 951-956,
337   1954.
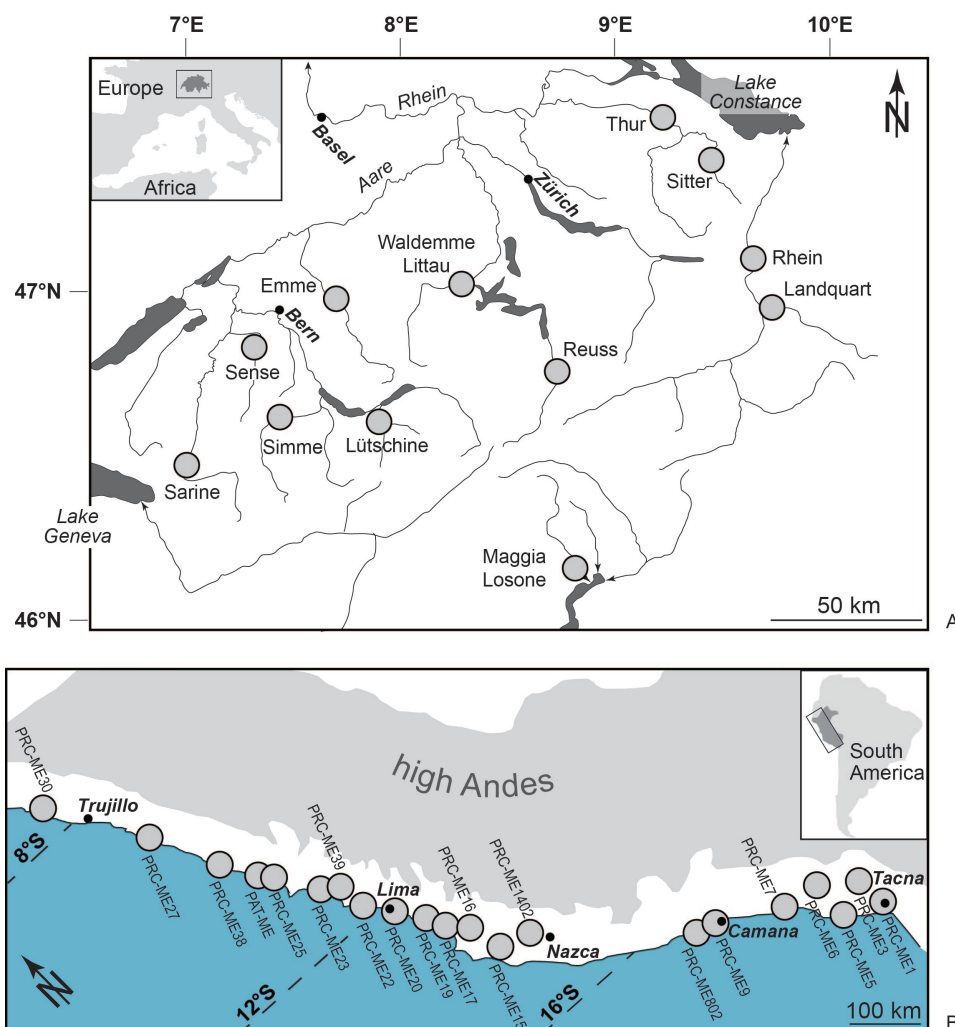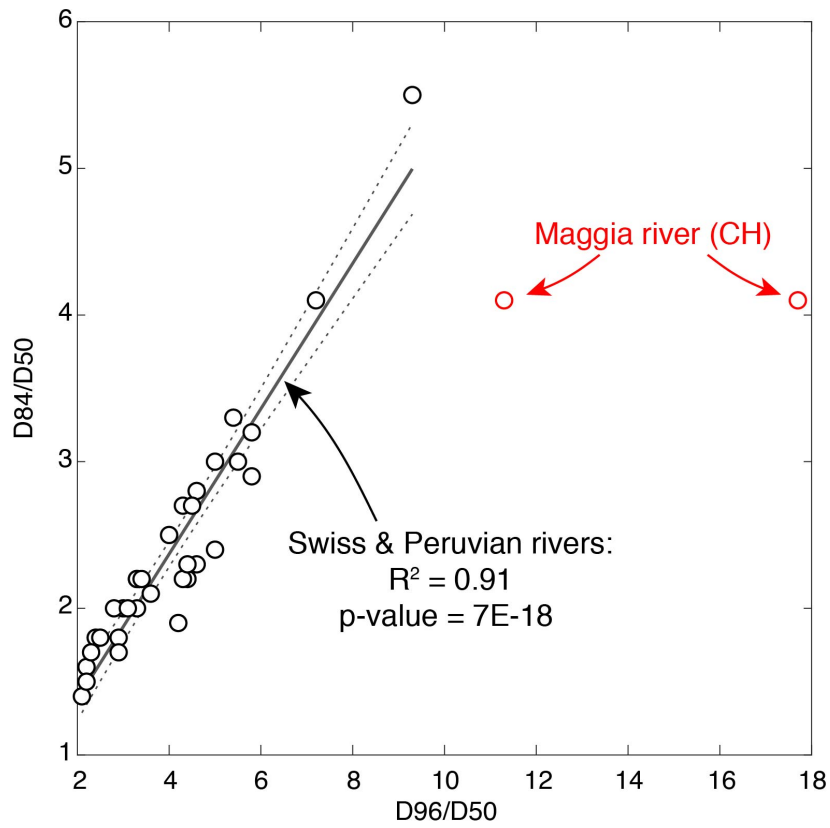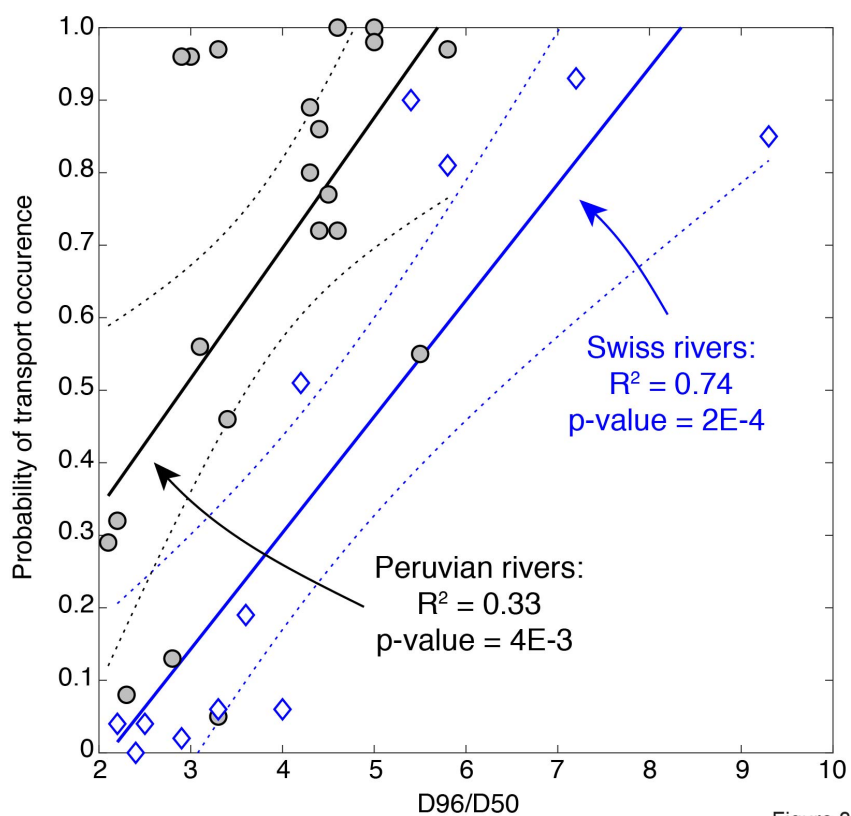
338
339

340
341
Figure 1

Figure 2

342
343

Figure 3

TABLE 1. GRAIN SIZE, CHANNEL METRICS, SHEAR STRESSES AND RELATIVE TRANSPORT TIME

Id	River	Site coordinates Latitude (DD WGS84)	Site coordinates Longitude (DD WGS84)	Channel width along reach (m)	Reach gradient (m/m)	Qmed: Mean annual water discharge (m3/s)	Standard deviation of Qmed (m3/s)	Unit discharge (Q/W; m2/s)	D50 (m)	D84 (m)	D96 (m)	D96/D50	D84/D50	Critical Sheer (median) (Pa)	Critical Sheer (16th%) (Pa)	Critical Sheer (84th%) (Pa)	Sheer stress in response to Qmed (Pa)	Sheer stress in response to Qmed (16th%) (Pa)	Sheer stress in response to Qmed (84th%) (Pa)	Relative transport time for Qmed and the D84 as threshold
1	Emme*	46.96	7.75	30	0.007	11.9	2.5	0.4	0.009	0.029	0.052	5.8	3.2	21	15	29	30	23	39	81%
2	Landquart*	46.98	9.61	32	0.018	24.1	5.1	0.8	0.025	0.083	0.135	5.4	3.3	60	42	82	102	79	130	90%
3	Waldemme Littau*	47.07	8.28	27	0.011	15.5	2.8	0.6	0.009	0.050	0.084	9.3	5.5	36	26	50	55	42	69	85%
4	Reuss*	46.88	8.62	48	0.007	42.9	4.7	0.9	0.009	0.037	0.064	7.2	4.1	27	19	37	48	38	60	93%
5	Maggia Losone II*	46.17	8.77	84	0.005	22.7	10.8	0.3	0.011	0.046	0.127	11.3	4.1	33	23	46	19	12	26	11%
6	Maggia Losone I*	46.17	8.77	22	0.005	22.7	10.8	1.0	0.008	0.033	0.140	17.7	4.1	24	17	33	39	26	53	83%
7	Rhein	47.01	9.30	92	0.002	167.5	24.5	1.8	0.070	0.128	0.169	2.4	1.8	92	65	127	26	20	32	0%
8	Sarine	46.36	7.05	24	0.004	21.0	3.9	0.9	0.049	0.080	0.108	2.2	1.6	58	41	80	27	21	35	4%
9	Lütschine	46.38	7.53	32	0.007	19.0	1.7	0.6	0.061	0.111	0.153	2.5	1.8	80	56	110	39	31	49	4%
10	Thur	47.30	9.12	52	0.002	37.9	6.8	0.7	0.024	0.045	0.069	2.9	1.8	32	23	45	13	10	17	2%
11	Simme	46.39	7.27	15	0.014	12.0	1.8	0.8	0.062	0.119	0.263	4.2	1.9	86	61	118	87	68	109	51%
12	Sitter	47.24	9.19	26	0.005	10.2	1.6	0.4	0.028	0.064	0.094	3.3	2.2	46	33	64	24	19	30	6%
13	Kander	46.39	7.40	26	0.009	20.0	2.3	0.8	0.054	0.116	0.193	3.6	2.1	84	59	115	58	46	72	19%
14	Sense*	46.89	7.35	24	0.005	8.7	1.7	0.4	0.024	0.060	0.096	4.0	2.5	43	31	60	22	17	28	6%
15	PRC-ME1#	-18.12	-70.33	6	0.015	3.4	0.8	0.6	0.023	0.060	0.100	4.3	2.7	45	32	62	76	58	97	89%
16	PRC-ME3#	-17.82	-70.51	6	0.013	4.0	5.0	0.7	0.025	0.055	0.110	4.4	2.2	40	28	55	83	46	126	86%
17	PRC-ME5#	-17.29	-70.99	7	0.018	3.4	1.0	0.5	0.026	0.051	0.078	3.0	2.0	37	26	51	82	61	107	96%
18	PRC-ME6#	-17.03	-71.69	26	0.051	38.1	37.8	1.5	0.015	0.036	0.075	5.0	2.4	26	18	36	432	244	643	100%
19	PRC-ME802#	-16.34	-72.13	15	0.019	30.1	21.7	2.0	0.020	0.060	0.100	5.0	3.0	43	31	60	193	116	278	98%
20	PRC-ME7#	-16.51	-72.64	100	0.005	68.4	52.7	0.7	0.052	0.087	0.120	2.3	1.7	63	44	86	31	18	45	8%
21	PRC-ME9#	-16.42	-73.12	70	0.004	91.1	82.2	1.3	0.048	0.068	0.100	2.1	1.4	49	35	68	37	21	54	29%
22	PRC-ME1402#	-15.85	-74.26	3	0.014	20.4	29.9	6.8	0.013	0.030	0.060	4.6	2.3	22	15	30	336	182	510	100%
23	PRC-ME15#	-15.63	-74.64	23	0.003	12.1	16.7	0.5	0.029	0.064	0.096	3.3	2.2	46	33	64	19	10	29	5%
24	PRC-ME16#	-13.73	-75.89	20	0.013	13.6	17.8	0.7	0.030	0.066	0.130	4.3	2.2	48	34	66	85	47	129	80%
25	PRC-ME17#	-13.47	-76.14	5	0.010	10.1	14.8	2.0	0.013	0.038	0.076	5.8	2.9	28	19	38	126	68	191	97%
26	PRC-ME19#	-13.12	-76.39	60	0.010	26.4	25.9	0.4	0.020	0.046	0.088	4.4	2.3	33	23	46	49	28	72	72%
27	PRC-ME20#	-12.67	-76.65	22	0.008	8.2	9.8	0.4	0.016	0.048	0.088	5.5	3.0	35	25	48	38	21	57	55%
28	PRC-ME22#	-12.25	-76.89	5	0.022	3.7	4.3	0.7	0.030	0.050	0.088	2.9	1.7	36	26	50	141	78	212	96%
29	PRC-ME39#	-11.79	-76.99	40	0.018	4.9	5.1	0.1	0.053	0.105	0.150	2.8	2.0	76	54	104	42	24	63	13%
30	PRC-ME23#	-11.61	-77.24	20	0.010	8.9	7.8	0.4	0.055	0.083	0.120	2.2	1.5	60	42	82	48	27	70	32%
31	PRC-ME25#	-11.07	-77.59	5	0.012	3.8	4.6	0.8	0.028	0.077	0.130	4.6	2.8	56	39	77	82	45	124	72%
32	PAT-ME#	-10.72	-77.77	30	0.014	30.9	24.3	1.0	0.018	0.036	0.060	3.3	2.0	26	18	36	102	60	148	97%
33	PRC-ME38#	-10.07	-78.16	15	0.004	9.8	12.7	0.7	0.017	0.034	0.052	3.1	2.0	25	17	34	28	15	42	56%
34	PRC-ME27#	-8.97	-78.62	40	0.005	96.1	67.7	2.4	0.020	0.054	0.090	4.5	2.7	39	27	54	61	37	87	77%
35	PRC-ME30#	-7.32	-79.48	40	0.007	25.4	27.7	0.6	0.029	0.063	0.100	3.4	2.2	45	32	63	44	24	65	46%

Italic=Swiss Rivers, plain=Peruvian Rivers
Water discharge data from the Swiss Federal Office for the Environment (FOEN: www. hydrodaten.admin.ch). Reported values represent discharges monitored over the period 1990-2011; Except for the Rhein (1977-1990).
Water discharge and drainage basin size data from the Peruvian Rivers is taken from Reber et al. (2017) and Litty et al. (2017)
#The grain size data from the Peruvian streams is taken from Litty et al. (2017)
*The grain size data, channel width and gradient data from the Emme, Landquart, Reuss, Maggia and Sense Rivers is taken from Litty and Schlunegger (2017)